Journal of Zhejiang University-SCIENCE C (Computers & Electronics)
ISSN 1869-1951 (Print); ISSN 1869-196X (Online)
www.zju.edu.cn/jzus; www.springerlink.com
E-mail: jzus@zju.edu.cn

Determination of inter-satellite relative position using X-ray pulsars*

Da-jun FENG[1,2], Lu-ping XU[†‡1,2], Hua ZHANG[1,2], Shi-bin SONG[1,2]

([1]*School of Electronic Engineering, Xidian University, Xi'an 710071, China*)

([2]*Institute of Astronautics and Aeronautics, Xidian University, Xi'an 710071, China*)

[†]E-mail: xd203@yahoo.com.cn

Received June 9, 2012; Revision accepted Jan. 1, 2013; Crosschecked Jan. 4, 2013

Abstract: Pulsars are rapidly rotating neutron stars that generate pulsed electromagnetic radiation. A new method for inter-satellite relative position determination between a global navigation satellite system (GNSS) and spacecraft using X-ray pulsars is proposed in this paper. The geometric model of this method is formulated, and two different resolution algorithms are introduced and analyzed. The phase cycle ambiguity resolution is investigated, and a new strategy is proposed and formulated. Using the direct vector parameters of the pulsar, geometric dilution of precision (GDOP) is studied. It is shown that this method has advantages of simplicity and efficiency, and is able to eliminate the clock errors. The analytical results are verified numerically via computer simulations.

Key words: Pulsar navigation, Position determination, Phase cycle ambiguity, Geometric dilution of precision (GDOP)
doi:10.1631/jzus.C12a0142 **Document code:** A **CLC number:** V448.21

1 Introduction

Pulsars, especially milli-second pulsars, have come to represent perhaps the most stable clocks ever devised, rivaling or exceeding in performance our best arrays of atomic time standards here on earth considering long time stability (Backer and Hellings, 1986; Taylor, 1992). As a result, X-ray pulsars can be used as a kind of 'natural lighthouse' to provide a novel technique to determine spacecraft time, position, velocity, and attitude. Recently, researchers have studied several aspects of utilizing X-ray pulsars for both absolute navigation (Emadzadeh and Speyer, 2010; Tartaglia *et al*., 2011) and relative navigation (Sheikh *et al*., 2007; Emadzadeh and Speyer, 2011).

For absolute navigation, it is necessary to create phase timing models, so that navigation algorithms can compare the measured time of arrival (TOA) to the expected TOA, and the difference can be translated directly to a position error of the spacecraft in the signal transmission direction of the pulsar being observed. Almost immediately after its proposal, spacecraft navigation using X-ray pulsars yielded surprising results considering its independence and self-determination in any earth orbit as well as in interplanetary and interstellar spaces. The accuracy of pulse timing models depends significantly on whether X-ray photons from pulsars continue to match the short-term timing models' forecast rotation rates, and plays a crucial part in X-ray pulsar based navigation. Unfortunately, although X-ray pulsars show a high long-term stability, two main forms of timing irregularity, i.e., glitches (nearly instantaneous changes in the pulse period) and timing noise (the stochastic wandering of the pulse phase), make the short-term phase prediction of the pulsars' rotation imprecise and uncertain. In addition, some young pulsars are subjected to irregular slow-down rate, which also influences the short-term forecast accuracy (Backer and Hellings, 1986; Taylor, 1992). Moreover, effects of pulsar proper motion, binary pulsars, accretion onto pulsar surface, astrospace particle clouds, gravitation

‡ Corresponding author
* Project supported by the National Natural Science Foundation of China (No. 61172138) and the Open Fund of Key Laboratory of Precision Navigation and Timing Technology, National Time Service Center, Chinese Academy of Sciences (No. 2012PNTT02)

waves outside the solar system, etc., increase the difficulty of an exact phase prediction. Therefore, in practice, besides from being developed from years of observations at ground-based radio telescopes or satellite-based X-ray detectors, credible phase timing models are supposed to be supervised and updated. Alternatively, it is important for X-ray pulsars to work in unison with other space navigation systems, so as to make spacecraft navigation farther and more reliable (Woodfork *et al.*, 2005; Fang and Ning, 2009).

Once, a global navigation satellite system (GNSS), such as the global positioning system (GPS), has revolutionized the navigation of everything, such as terrestrial cars, maritime ships, and aerial flying planes. Nevertheless, GNSS does not provide a satisfactory solution to the navigation of spacecraft outside the orbits of the GNSS constellation. Therefore, it is significant to extend the navigation capability of GNSS beyond its constellation orbits using X-ray pulsars. In addition, positions determined relative to GNSS satellites can provide some additional information for TOA phase models used in X-ray pulsar based navigation to real-time automatic correction.

In this article, we present a new method for inter-satellite relative position determination between GNSS satellites and spacecraft using X-ray pulsars. Actually, several relative navigation strategies have been suggested in recent years. For instance, Sheikh *et al.* (2007) pointed out that the periodic celestial body including X-ray pulsars can be used for relative navigation in many applications, which require only relative range information such as spacecraft formation. Using the pulsar measurements, Emadzadeh and Speyer (2011) proposed a recursive algorithm for relative navigation between two spacecraft. Xiong *et al.* (2008) studied an autonomous navigation technique based on X-ray pulsars for a satellite in a constellation using time difference of arrival (TDOA). Unlike Xiong *et al.* (2008) and Emadzadeh and Speyer (2011), the proposed method suggests using GNSS satellite to retransmit the TOA of the X-ray photon sequential in real time. There are two main features of this method. First, it can eliminate the clock error due to time synchronization; second, it can obtain 3D relative positions, and the absolute position can also be resolved using the GNSS satellite position which is known exactly. In this paper, the geometric model of this method is formulated, and two different resolution algorithms are introduced and analyzed. Then, a new full period relation formula is presented for pulse phase cycle ambiguity resolution. The technique for correction of relative movement between spacecraft and GNSS satellites is introduced, and the method for TOA phase model correction using the relative position is specified. Finally, effects of geometric dilution of precision (GDOP) in inter-satellite relative position determination, using X-ray pulsars, are analyzed.

2 Algorithm for inter-satellite relative position determination using X-ray pulsars

2.1 Principles and formulations

It is assumed that both X-ray detectors and deep-space antennas are set onto spacecraft and GNSS satellites, respectively. Although current GNSS does not have this type of equipment, it can be equipped in the future GNSS, such as the next generation of GPS satellites or the Beidou-2 satellite developed by China. For simplicity, we take GPS as an example in the following paragraphs.

The on-satellite detector detects the X-ray photons from X-ray pulsars and records their TOA, while the X-ray photons hit the detector material based on the atomic clock. Then, as shown in Fig. 1, a time sequence is formed using time bin Δt to sample the TOA and summing the number of photons within a time bin. Immediately, the onboard antenna transmits the time sequence successively using a communication channel. It should be noted that the time bin size determines the timing resolution of pulsar signals, and causes time delay in the process of photon reception and signal retransmission (Sheikh and Pines, 2006). Pulsars and their parameters are shown in Table 1, where α is the right ascension, β is the declination, p is the period, and F_x is the flux intensity (Sheikh, 2005). We assume the effective area is 1 m^2 and a bin length of 1 μs. In the simulation, the TOA measuring method (Zhang and Xu, 2011) is used to generate the position variance error.

Both X-ray photons from X-ray pulsars and electromagnetic waves carrying the photons' arrival time sequence from GPS satellites can be received by spacecraft, so both the pulse from an X-ray pulsar and its copy with phase delay will be obtained. Phase interval between the two arrivals of the same pulse represents the sum of the distance between the spacecraft and the GPS satellite in the direction of the X-ray pulsar being observed, and the linear distance between them. The distance relation is shown in Fig. 2.

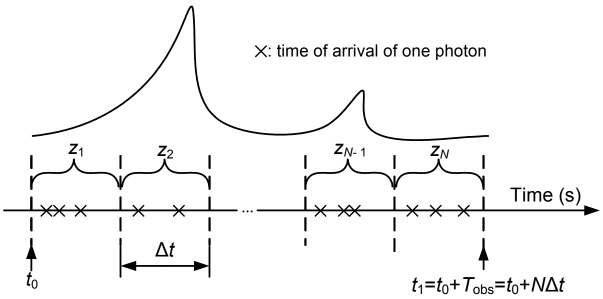

Fig. 1 Photons and time bin

Table 1 Pulsars and their parameters

Pulsar	α (°)	β (°)	p (s)	F_x (ph·s /cm^2)
B0531+21	83.63	22.01	0.03340	1.54
B1821-24	276.13	−24.87	0.00305	1.93×10^{-4}
B1937+21	294.92	21.58	0.00156	4.99×10^{-5}
J1751-305	359.18	−1.91	0.00230	1.17×10^{-9}

α: right ascension; β: declination; p: period; F_x: flux intensity

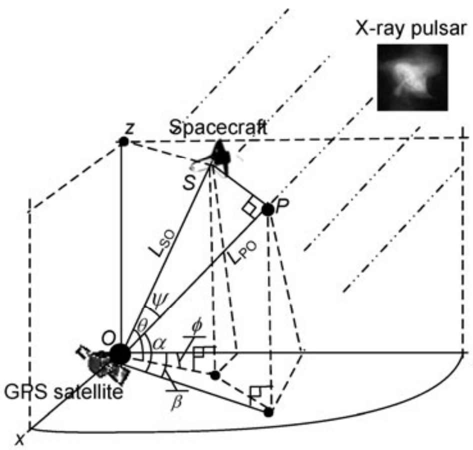

Fig. 2 Geometric layout of inter-satellite relative position determination

It is the time interval measured by the clock in the spacecraft instead of the exact time read from the clock in the GPS satellites and the spacecraft that is used to calculate the relative position after being translated to a common inertial reference system. Therefore, the result is dependent on the stability of the on-satellite clocks but independent of the difference between the exact clock time of the GPS satellite and the spacecraft.

X-ray pulsars are very far away from the solar system, so the line-of-sight to the emitting source is considered constant within the solar system. Let L_{SO} be the distance between S and O and L_{PO} be the distance between the GPS satellite and the spacecraft in the direction of the pulsar being observed. Furthermore, C is the speed of light and ΔT_i is the time interval while the X-ray pulsar i is observed. Then, the relation between the distance sum and the time interval is expressed as

$$L_{PO}+L_{SO}=C\Delta T, \tag{1}$$

$$L_{SO}\cos\psi=L_{PO}, \tag{2}$$

where ψ is the angle between directions of the spacecraft and the X-ray pulsar in the polar coordinate system centered by the GPS satellite. ψ can be expressed as

$$\cos\psi=\cos\alpha\cos\beta\cos\theta\cos\phi+\cos\alpha\sin\beta\cos\theta\sin\phi+\sin\alpha\sin\theta, \tag{3}$$

$$0\le\psi\le 90°, \tag{4}$$

where θ is the angle from the x-y coordinate plane to the direction of the spacecraft in the polar coordinate system centered by the GPS satellite, and ϕ is the angle from the x-axis to the direction of the projection on the x-y coordinate plane by the spacecraft. To describe the direction of X-ray pulsars, let α_i be the right ascension (J2000) (°) of pulsar i and β_i be the declination (J2000) (°) of pulsar i.

A solution to L_{SO} can be expressed as

$$L_{SO}=\frac{C\Delta T}{1+\cos\psi}=C\Delta T\cdot(1+|\cos\alpha\cos\beta\cos\theta\cos\phi+\cos\alpha\sin\beta\cos\theta\sin\phi+\sin\alpha\sin\theta|)^{-1}, \tag{5}$$

where

$$C\Delta T/2\le L_{SO}\le C\Delta T, \tag{6}$$

$$\cos(\varphi-\beta)\ge-\tan\alpha\tan\theta. \tag{7}$$

Thus, the relation between the position (x, y, z) relative to the GPS satellite and the time interval ΔT can be expressed as

$$\cos\alpha\cos\beta\cdot x+\cos\alpha\sin\beta\cdot y+\sin\alpha\cdot z+\sqrt{x^2+y^2+z^2}=C\Delta T. \quad (8)$$

It can be seen from Eq. (8) that the spacecraft is located on a curved surface in the polar coordinate system centered by the GPS satellite when one X-ray pulsar is observed.

Observations of at least three X-ray pulsars can be utilized to provide a solution to the 3D spacecraft position. The location equations can be expressed as

$$\begin{cases}\cos\alpha_1\cos\beta_1\cdot x+\cos\alpha_1\sin\beta_1\cdot y+\sin\alpha_1\cdot z+r\\ \quad =C\Delta T_1=\rho_1(x,y,z),\\ \cos\alpha_2\cos\beta_2\cdot x+\cos\alpha_2\sin\beta_2\cdot y+\sin\alpha_2\cdot z+r\\ \quad =C\Delta T_2=\rho_2(x,y,z),\\ \cos\alpha_3\cos\beta_3\cdot x+\cos\alpha_3\sin\beta_3\cdot y+\sin\alpha_3\cdot z+r\\ \quad =C\Delta T_3=\rho_3(x,y,z),\end{cases} \quad (9)$$

where $r=\sqrt{x^2+y^2+z^2}$ is the value of L_{SO}.

Assuming the approximate position of spacecraft to be $(\hat{x},\hat{y},\hat{z})$, we have

$$\begin{cases}x=\hat{x}+\Delta x,\\ y=\hat{y}+\Delta y,\\ z=\hat{z}+\Delta z,\end{cases} \quad (10)$$

where Δx, Δy, and Δz are the differences between the real position and the approximate position.

Let ε be the iteration precision. Using linear iteration with the precision $\sqrt{\Delta x^2+\Delta y^2+\Delta z^2}\le\varepsilon$, we can obtain (x, y, z) by

$$\Delta\boldsymbol{\rho}=\left[\Delta\rho_1,\Delta\rho_2,\Delta\rho_3\right]^{\mathrm{T}}=\boldsymbol{\rho}-\hat{\boldsymbol{\rho}}, \quad (11)$$

$$\Delta\boldsymbol{x}=\left[\Delta x,\Delta y,\Delta z\right]^{\mathrm{T}}, \quad (12)$$

$$\boldsymbol{H}=\begin{pmatrix}\cos\alpha_1\cos\beta_1+\frac{\hat{x}}{\hat{r}} & \cos\alpha_1\sin\beta_1+\frac{\hat{y}}{\hat{r}} & \sin\alpha_1+\frac{\hat{z}}{\hat{r}}\\ \cos\alpha_2\cos\beta_2+\frac{\hat{x}}{\hat{r}} & \cos\alpha_2\sin\beta_2+\frac{\hat{y}}{\hat{r}} & \sin\alpha_2+\frac{\hat{z}}{\hat{r}}\\ \cos\alpha_3\cos\beta_3+\frac{\hat{x}}{\hat{r}} & \cos\alpha_3\sin\beta_3+\frac{\hat{y}}{\hat{r}} & \sin\alpha_3+\frac{\hat{z}}{\hat{r}}\end{pmatrix}, \quad (13)$$

where $\hat{r}=\sqrt{\hat{x}^2+\hat{y}^2+\hat{z}^2}$. Then, we can obtain $\Delta\boldsymbol{x}=\boldsymbol{H}^{-1}\Delta\boldsymbol{\rho}$. Using Eq. (10), we can then obtain (x, y, z). If $(\Delta x, \Delta y, \Delta z)$ satisfies $\sqrt{\Delta x^2+\Delta y^2+\Delta z^2}\le\varepsilon$, (x,y,z) will be the resolution; otherwise, we make (x, y, z) be the new $(\hat{x},\hat{y},\hat{z})$ to repeat the process until the iteration precision is satisfied.

Theoretically, only three X-ray pulsars are needed to determine the spacecraft position (x, y, z) relative to the GPS satellite, while more X-ray pulsars can actually improve its precision. In this case, we use a least square method to resolve the position.

Suppose we have M (M>3) X-ray pulsars available. Then $\boldsymbol{H}$ will be a matrix as follows:

$$\boldsymbol{H}=\begin{pmatrix}\cos\alpha_1\cos\beta_1+\frac{\hat{x}}{\hat{r}} & \cos\alpha_1\sin\beta_1+\frac{\hat{y}}{\hat{r}} & \sin\alpha_1+\frac{\hat{z}}{\hat{r}}\\ \cos\alpha_2\cos\beta_2+\frac{\hat{x}}{\hat{r}} & \cos\alpha_2\sin\beta_2+\frac{\hat{y}}{\hat{r}} & \sin\alpha_2+\frac{\hat{z}}{\hat{r}}\\ \cos\alpha_3\cos\beta_3+\frac{\hat{x}}{\hat{r}} & \cos\alpha_3\sin\beta_3+\frac{\hat{y}}{\hat{r}} & \sin\alpha_3+\frac{\hat{z}}{\hat{r}}\\ \cos\alpha_4\cos\beta_4+\frac{\hat{x}}{\hat{r}} & \cos\alpha_4\sin\beta_4+\frac{\hat{y}}{\hat{r}} & \sin\alpha_4+\frac{\hat{z}}{\hat{r}}\\ \vdots & \vdots & \vdots\end{pmatrix}. \quad (14)$$

Then, we will have $\Delta\boldsymbol{x}=(\boldsymbol{H}^{\mathrm{T}}\boldsymbol{H})^{-1}\Delta\boldsymbol{\rho}$, and

$$\begin{pmatrix}x\\ y\\ z\end{pmatrix}=\begin{pmatrix}\hat{x}\\ \hat{y}\\ \hat{z}\end{pmatrix}+\begin{pmatrix}\Delta x\\ \Delta y\\ \Delta z\end{pmatrix}. \quad (15)$$

Similarly, if $(\Delta x, \Delta y, \Delta z)$ satisfies $\sqrt{\Delta x^2+\Delta y^2+\Delta z^2}\le\varepsilon$, (x, y, z) will be the resolution; otherwise, we make (x, y, z) be the new $(\hat{x},\hat{y},\hat{z})$ to repeat the process until we obtain the resolution.

In addition, using several GPS satellites synchronously is another way to improve the inter-satellite relative precision. Solution optimization using several GPS satellites is shown in Fig. 3.

After the spacecraft position (x, y, z) relative to the GPS satellite is calculated, the position in a common reference frame, such as the solar system barycenter frame, can be reckoned up using the precise GPS constellation ephemeris data.

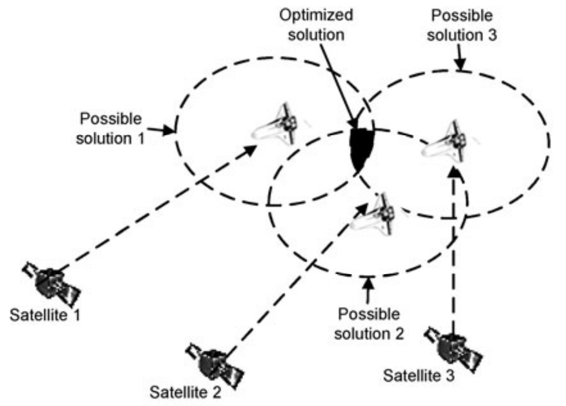

Fig. 3 Solution optimization using several GPS satellites

We also find that GNSS can be used to measure the distance between GNSS satellites and spacecraft, but the length of the baseline and the orbit limit its GDOP. In the proposed method, pulsars can improve the GDOP greatly because of their uniform distribution in the celestial sphere. In Section 5, we give the details.

2.2 Simulation results

As shown in Fig. 4, we choose 100 sets of α and β to resolve positions using the linear iteration method. α is the declination (J2000) of a pulsar and β is the right ascension of a pulsar. In each set, there are three α and β, which represent three different X-ray pulsar locations. The 100 sets of α and β can also be divided into 10 groups. In each group, α is the same and β varies. Among different groups, β remains unchanged and α varies.

Similarly, in Fig. 5 we choose 100 sets of α and β to resolve positions with the least square method. In each set, there are four α and β, which represent four different X-ray pulsar locations. The 100 sets of α and β can also be divided into 10 groups. In each group, α is the same and β varies. Among different groups, β remains unchanged and α varies.

Ten white Gaussian noises with different degrees of power are added to ΔT to simulate noises. The power of white Gaussian noise in one group is larger than that of its former one. With α and β selected in Figs. 4 and 5, we use linear iteration method and least square method respectively to resolve the user's positions in each group. Then, we compare the results with the positions resolved without noise and calculate the variance of position deviation.

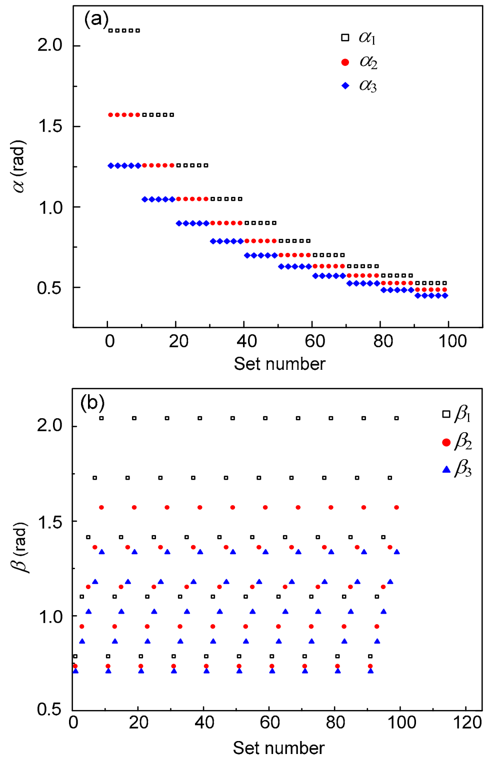

Fig. 4 Values of α (a) and β (b) for the linear iteration method

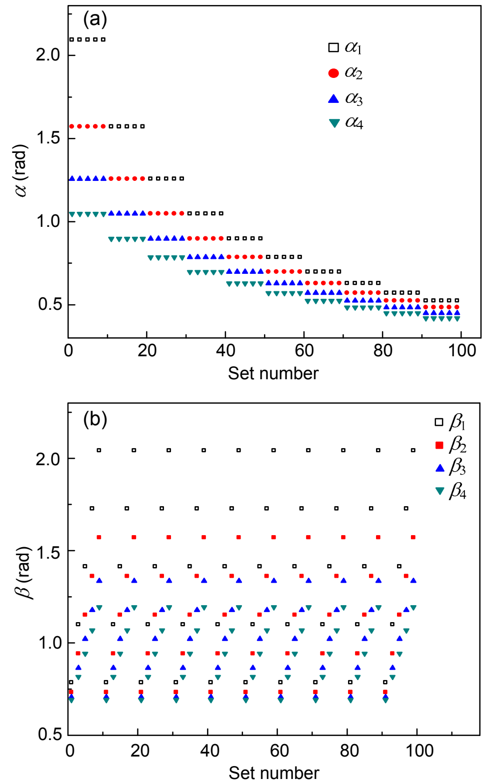

Fig. 5 Values of α (a) and β (b) for the least square method

From Fig. 6, we can see that the variance of position deviation of the least square method is smaller than that of the linear iteration method, which means that the least square method has a better resolution precision over the linear iteration method and a better noise resistance under the same situation. When the power of noise is small, the variance of position deviation is small as well. But, when the power of noise becomes large, the variance of position deviation will greatly increase and become too large to satisfy the resolution precision.

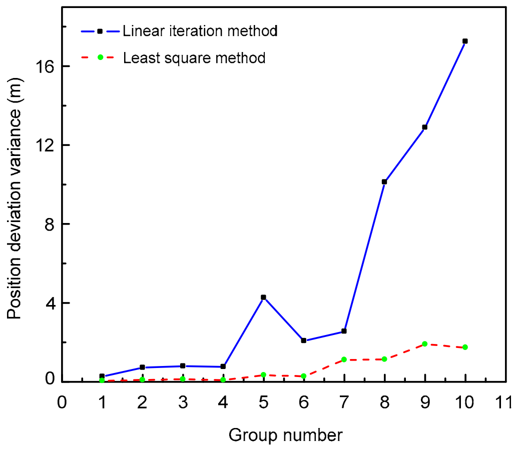

Fig. 6 Position deviation variances using the least square method and the linear iteration method

3 Pulse phase cycle ambiguity resolution

Comparison of two integrated pulses does not determine the entire distance between the GPS satellites and the spacecraft unless the number of full pulse cycles between both of the time arrivals is also known, which means that pulse cycles are ambiguous (Fig. 7). Additional methods must be developed to resolve these ambiguous cycles, so that their true relative positions can be determined. The basic method to pulse phase cycle ambiguity resolution in X-ray pulsar based navigation was described by Sala *et al.* (2004) and Sheikh (2005). It relies on the fact that for a given fully determined set of phase measurements from separate pulsars, there is one unique position in the 3D space that satisfies all the measurements (Moyer, 2003; Sala *et al.*, 2004; Sheikh, 2005; Zhang *et al.*, 2011b). Therefore, for the resolution of pulse phase ambiguity, cycle sets should be generated after a search space is established. Then, testing these candidate sets one by one in location equations is implemented until the most likely one is selected out.

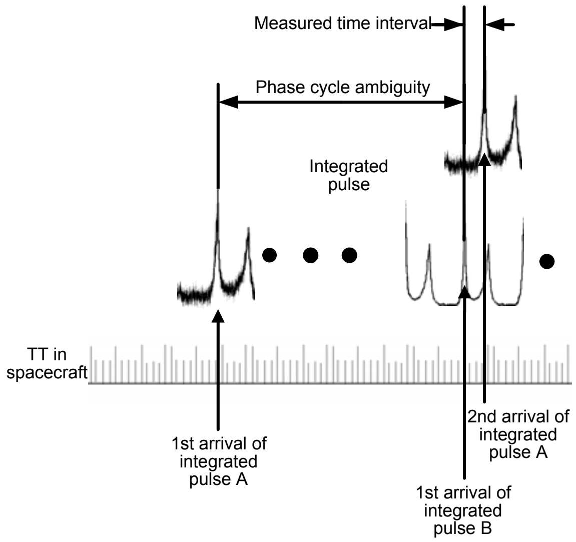

Fig. 7 Pulse phase cycle ambiguity

It is a new relation of full pulse cycle numbers that is presented in this article, not location equations that are used for pulse phase cycle ambiguity resolution.

Let m_i be the number of full pulse cycles in ΔT_i, T_i be the period of pulse signal from X-ray pulsar i, and ΔR_i be the residual of ΔT_i. When the relative distance r is calculated, Eq. (9) can be expressed as

$$\cos\alpha_1\cos\beta_1\cdot x+\cos\alpha_1\sin\beta_1\cdot y+\sin\alpha_1\cdot z=l_1, \quad (16a)$$
$$\cos\alpha_2\cos\beta_2\cdot x+\cos\alpha_2\sin\beta_2\cdot y+\sin\alpha_2\cdot z=l_2, \quad (16b)$$
$$\cos\alpha_3\cos\beta_3\cdot x+\cos\alpha_3\sin\beta_3\cdot y+\sin\alpha_3\cdot z=l_3, \quad (16c)$$
$$\cos\alpha_4\cos\beta_4\cdot x+\cos\alpha_4\sin\beta_4\cdot y+\sin\alpha_4\cdot z=l_4, \quad (16d)$$

where $l_i=C\Delta T_i-r=C(\Delta R_i+m_iT_i)-r$, i=1, 2, 3, 4. It can be seen that if the relative distance r is determined, the spacecraft is located at the point of intersection of multiple planes determined by X-ray pulsars being observed.

A value $\boldsymbol{X}_1(x_1, y_1, z_1)$ of the spacecraft position relative to the GPS satellite can be worked out with m_i unknown using Eqs. (16a), (16b), and (16c). If Eq. (16c) is replaced by Eq. (16d), another value $\boldsymbol{X}_2(x_2, y_2, z_2)$ with additional information can be worked out with m_i unknown. It is evident that the more likely candidate set $[m_1, m_2, m_3, m_4]$ should at least satisfy

$$E(\boldsymbol{X}_1-\boldsymbol{X}_2)^2<\boldsymbol{\xi}, \tag{17}$$

where $\boldsymbol{\xi}$ is the variance of the position error caused by time interval noise. x_1 in vector $\boldsymbol{X}_1$ can be expressed as

$$x_1=\frac{l_1X_{\mathrm{B}}+l_3X_{\mathrm{C}}+l_2X_{\mathrm{D}}}{X_{\mathrm{A}}}, \tag{18}$$

where

$$\begin{aligned}X_{\mathrm{A}}=&X_{\mathrm{B}}\cos\alpha_1\cos\beta_1+X_{\mathrm{C}}\cos\alpha_3\cos\beta_3\\&+X_{\mathrm{D}}\cos\alpha_2\cos\beta_2,\end{aligned} \tag{19}$$

$$X_{\mathrm{B}}=\cos\alpha_3\sin\beta_3\sin\alpha_2-\cos\alpha_2\sin\beta_2\sin\alpha_3, \tag{20}$$

$$X_{\mathrm{C}}=\cos\alpha_2\sin\beta_2\sin\alpha_1-\cos\alpha_1\sin\beta_1\sin\alpha_2, \tag{21}$$

$$X_{\mathrm{D}}=\cos\alpha_1\sin\beta_1\sin\alpha_3-\cos\alpha_3\sin\beta_3\sin\alpha_1. \tag{22}$$

Just like x_1, x_2 to x_4 in vector $\boldsymbol{X}_2$ can be expressed as the similar form.

In a more strict condition, it should satisfy

$$(x_1-x_2)^2+(y_1-y_2)^2+(z_1-z_2)^2<|\xi|^2. \tag{23}$$

Then, we can build an equation as follows:

$$f(m_1,m_2,m_3,m_4)=(x_1-x_2)^2+(y_1-y_2)^2+(z_1-z_2)^2. \tag{24}$$

The partial derivative of f with respect to m_1 is zero when f arrives at its minimum value of zero, which can be expressed as

$$\frac{\partial\left((x_1-x_2)^2+(y_1-y_2)^2+(z_1-z_2)^2\right)}{\partial m_1}=0. \tag{25}$$

The relation of full pulse cycle numbers is reyielded by resolving

$$m_1W_1+m_2W_2+m_3W_3-m_4W_4=S, \tag{26}$$

where

$$\begin{aligned}
S=&C\Delta R_4U_4-C\Delta R_3U_3-C\Delta R_2U_2-C\Delta R_1U_1\\
&-r(U_4-U_3-U_2-U_1),\\
W_i=&CU_iT_i,\quad i=1,2,3,4,\\
U_1=&\frac{P_{\mathrm{B}}^{2}}{P_{\mathrm{A}}^{2}}+\frac{P_{\mathrm{B}}''^{2}}{P_{\mathrm{A}}''^{2}}+\frac{P_{\mathrm{B}}'^{2}}{P_{\mathrm{A}}'^{2}},\\
U_2=&\frac{P_{\mathrm{B}}P_{\mathrm{C}}}{P_{\mathrm{A}}^{2}}+\frac{P_{\mathrm{B}}''P_{\mathrm{C}}''}{P_{\mathrm{A}}''^{2}}+\frac{P_{\mathrm{B}}'P_{\mathrm{C}}'}{P_{\mathrm{A}}'^{2}},\\
U_3=&\frac{P_{\mathrm{B}}P_{\mathrm{D}}}{P_{\mathrm{A}}^{2}}+\frac{P_{\mathrm{B}}''P_{\mathrm{D}}''}{P_{\mathrm{A}}''^{2}}+\frac{P_{\mathrm{B}}'P_{\mathrm{D}}'}{P_{\mathrm{A}}'^{2}},\\
U_4=&\frac{P_{\mathrm{B}}P_{\mathrm{E}}}{P_{\mathrm{A}}^{2}}+\frac{P_{\mathrm{B}}''P_{\mathrm{E}}''}{P_{\mathrm{A}}''^{2}}+\frac{P_{\mathrm{B}}'P_{\mathrm{E}}'}{P_{\mathrm{A}}'^{2}},\\
P_{\mathrm{A}}=&\boldsymbol{X}_{\mathrm{A}}\cdot\boldsymbol{X}_{\mathrm{A}}',\\
P_{\mathrm{B}}=&\boldsymbol{X}_{\mathrm{B}}\cdot\boldsymbol{X}_{\mathrm{A}}'-\boldsymbol{X}_{\mathrm{B}}'\cdot\boldsymbol{X}_{\mathrm{A}},\\
P_{\mathrm{C}}=&\boldsymbol{X}_{\mathrm{D}}\cdot\boldsymbol{X}_{\mathrm{A}}'-\boldsymbol{X}_{\mathrm{D}}'\cdot\boldsymbol{X}_{\mathrm{A}},\\
P_{\mathrm{D}}=&\boldsymbol{X}_{\mathrm{C}}\cdot\boldsymbol{X}_{\mathrm{A}}',\\
P_{\mathrm{E}}=&\boldsymbol{X}_{\mathrm{C}}'\cdot\boldsymbol{X}_{\mathrm{A}},\\
X_{\mathrm{A}}'=&X_{\mathrm{B}}'\cos\alpha_1\cos\beta_1+X_{\mathrm{C}}'\cos\alpha_4\cos\beta_4\\
&+X_{\mathrm{D}}'\cos\alpha_2\cos\beta_2,\\
X_{\mathrm{B}}'=&\cos\alpha_4\sin\beta_4\sin\alpha_2-\cos\alpha_2\sin\beta_2\sin\alpha_4,\\
X_{\mathrm{C}}'=&\cos\alpha_2\sin\beta_2\sin\alpha_1-\cos\alpha_1\sin\beta_1\sin\alpha_2,\\
X_{\mathrm{D}}'=&\cos\alpha_1\sin\beta_1\sin\alpha_4-\cos\alpha_4\sin\beta_4\sin\alpha_1.
\end{aligned}$$

Actually, S is wandering stochastically around its mean value because of time interval noise. The detection threshold $\kappa\sigma$ (σ is standard deviation of S) is used to tell the validity of the candidate set $[m_1, m_2, m_3, m_4]$. Then, Eq. (27) is supplemented as follows:

$$m_1W_1+m_2W_2+m_3W_3-m_4W_4-S=\kappa\sigma, \tag{27}$$

where W_i is determined only by the characteristics of X-ray pulsars, including declination, right ascension, and period. S is determined by the measured values of ΔR_i and r and is independent of the characteristics of X-ray pulsars. Four X-ray pulsars are not always enough to pick out the most likely candidate set. Therefore, substitution of new X-ray pulsars into Eq. (27) is implemented. W_i and U_i can be calculated beforehand according to the sequence of X-ray pulsars being used. In the process of ambiguity resolution, candidate sets are tested one by one in Eq. (27) with X-ray pulsars and its corresponding U_i and W_i updated in the order determined beforehand, until the most likely one remains.

4 Correction of relative movement between the spacecraft and GPS satellites

In the process of inter-satellite relative position determination, GPS satellites and spacecraft are moving relatively (Fig. 8). The first arrival of an integrated pulse from the X-ray pulsar occurs while the spacecraft is arriving at the position *S*. The second arrival of the same integrated pulse from the GPS satellite occurs while the spacecraft arrives at *S*′. The difference between the actual time interval of these two arrivals and the one used in Eq. (1) will be caused by the relative movement between the GPS satellite and the spacecraft (Zhang *et al.*, 2011a). Different velocities between the GPS satellite and the spacecraft also result in different pulse signal frequencies, referred to as the Doppler effect.

The velocity of the spacecraft can be estimated according to frequency shift of the pulse signal from the X-ray pulsar, and the velocity of the GPS satellite can be estimated according to its ephemeris. Correction of the time interval can be implemented presumably using these velocities. Pulse integration should be implemented after the mission elapsed time (MET) is transformed to the barycentric dynamical time (TDB) system, and their observation positions are transferred uniformly to the position predicted according to the velocities, integration time piece, and time bins (Sala *et al.*, 2004; Zhang *et al.*, 2011b).

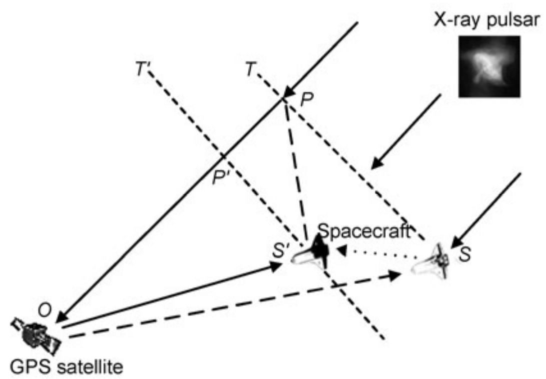

Fig. 8 Relative movement between the GPS satellite and the spacecraft

5 Analysis of geometric dilution of precision

GPS devices calculate a user's position using several spheres intersecting with a satellite at each sphere's center. Ideally, these spheres would intersect at exactly one point, causing there to be only one possible solution to the current location, but in reality, the intersection forms more of an oddly-shaped area because of the measurement error of the travel time of radio signals from satellites. Furthermore, the oddly-shaped area is larger when the GPS satellites are close together (Fig. 9), which is one of the handicaps to the navigation application in the interplanetary and interstellar space. However, X-ray pulsars are far and dispersive around the Earth. Intersectant curved surfaces used in inter-satellite relative position determination can be oriented by X-ray pulsars. Thus, its GDOP can be reduced by optimization of the intersection angles among curved surfaces by selecting more salutary X-ray pulsars (Fig. 10). Besides, one of the characteristics distinguishing X-ray pulsar based navigation from GNSS is that the GDOP does not change during the navigation period unless the pulsar used is replaced. Thus, a carefully selected pulsars set can improve the navigation.

It is known that GDOP is based upon the covariance matrices of the estimation error of the position solution. According to Sheikh (2005), for the 3×3 matrices, we have

$$\mathrm{GDOP}_{\mathrm{psr}} = \frac{\sqrt{\mathrm{tr}E(\Delta \boldsymbol{x}'\Delta \boldsymbol{x}'^{\mathrm{T}})}}{\Delta \boldsymbol{\rho}} = \sqrt{\mathrm{tr}(\boldsymbol{H}^{\mathrm{T}}\boldsymbol{H})^{-1}}.$$

As shown in Fig. 11, we choose 100 sets of α and β to check the influence of X-ray pulsar locations on GDOP. α is the declination (J2000) of a pulsar and β is the right ascension of a pulsar. In each set, there are four α and four β. The 100 sets of α and β can also be divided into 10 groups. In each group, β is constant and the differences between four α tend to become smaller. Among different groups, α remains the same and the differences between four β in one group become smaller as the group number grows.

Fig. 12 shows the influence of the locations of X-ray pulsars on GDOP. On one hand, in each group, as the differences of α tend to become smaller, GDOP increases accordingly on condition that β is fixed. On the other hand, the value of GDOP increases as the differences between the four β are getting smaller compared to the former group when α remains the same.

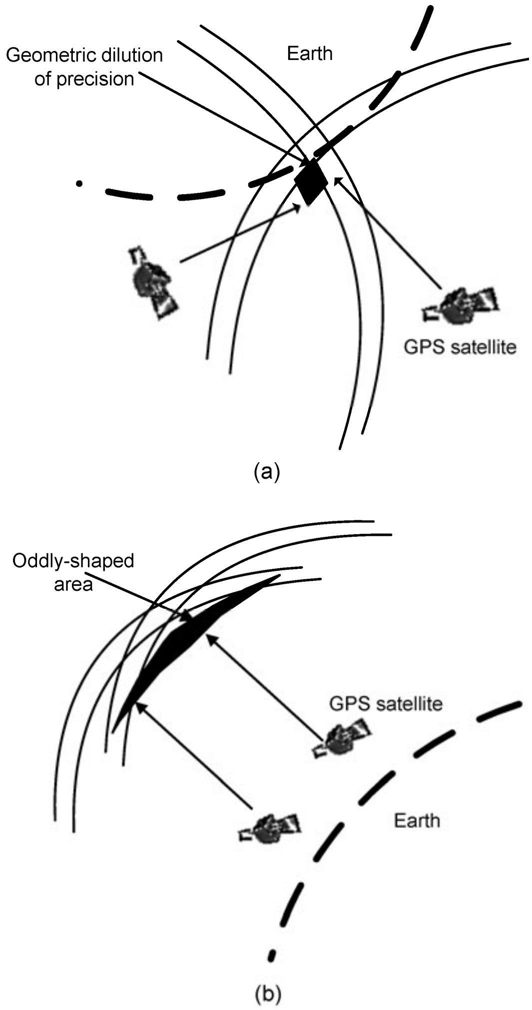

Fig. 9 Good (a) and bad (b) geometric dilution of precision of GPS satellite

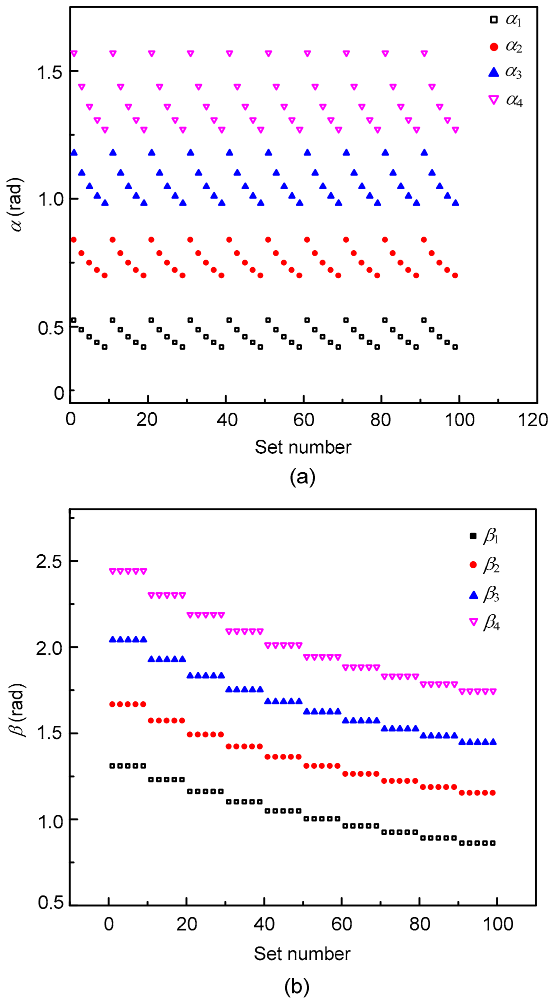

Fig. 11 Values of *α* (a) and *β* (b) selected to measure geometric dilution of precision

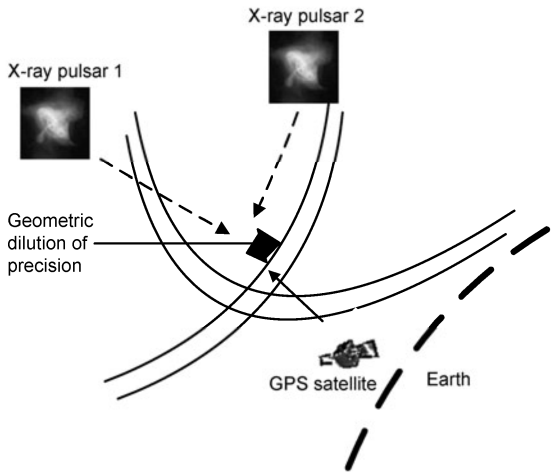

Fig. 10 Geometric dilution of precision of relative position determination using X-ray pulsars

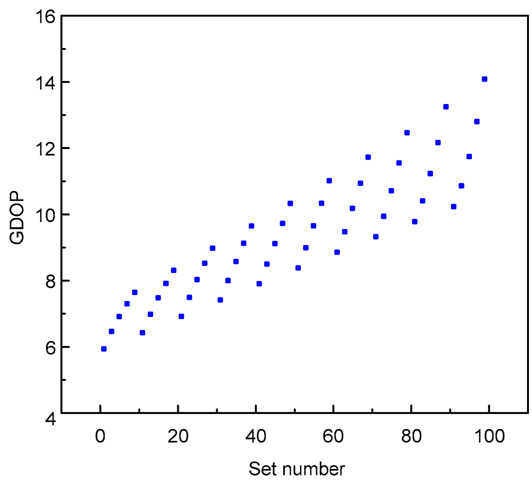

Fig. 12 Geometric dilution of precision influenced by locations of X-ray pulsars

Hence, when β is fixed, to obtain a comparatively small GDOP, α should be small and dispersive enough, and the differences between the four α should be relatively uniform. When α is fixed, β should be dispersive to get a relatively small GDOP. When the X-ray pulsars chosen are too close together, GDOP will be too large to satisfy the applications. By choosing salutary X-ray pulsars, the GDOP can effectively be reduced.

6 Conclusions

A new method for determination of inter-satellite relative position between GNSS and spacecraft using X-ray pulsars has been proposed in this paper. Using the formulated geometric model, the introduced linear iteration method and the least mean square method can both be used to resolve the relative position. Furthermore, it was observed that the latter one shows a better anti-noise ability. This method is also able to eliminate the clock error and resolve absolute position based on GNSS signals because of its retransmission mode. A full period number relation is established and deduced for pulse phase cycle ambiguity resolution. The new method provides high efficiency and easy reliability for engineering because of simplified formulae. The GDOP analysis shows that carefully selected pulsars can reduce GDOP effectively. Furthermore, pulsar-based navigation has a distinguishing characteristic where the GDOP is constant in all the navigation periods. Finally, in future work, we intend to apply the method to satellite formation and bring in iteration methods such as the Kalman filter.

References

Backer, D.C., Hellings, R.W., 1986. Pulsar timing and general relativity. *Ann. Rev. Astron. Astrophys.*, **24**(1):537-575. [doi:10.1146/annurev.aa.24.090186.002541]

Emadzadeh, A.A., Speyer, J.L., 2010. On modeling and pulse phase sstimation of X-ray pulsars. *IEEE Trans. Signal Process.*, **58**(9):4484-4495. [doi:10.1109/TSP.2010.2050479]

Emadzadeh, A.A., Speyer, J.L., 2011. Relative navigation between two spacecraft using X-ray pulsars. *IEEE Trans. Control Syst. Technol.*, **19**(5):1021-1035. [doi:10.1109/TCST.2010.2068049]

Fang, J.C., Ning, X.L., 2009. Installation direction analysis of star sensors by hybrid condition number. *IEEE Trans. Instrum. Meas.*, **58**(10):3576-3582. [doi:10.1109/TIM.2009.2018688]

Moyer, T.D., 2003. Formulation for Observed and Computed Values of Deep Space Network Data Types for Navigation. John Wiley & Sons, Inc., p.107-119. [doi:10.1002/0471728470]

Sala, J., Urruela, A., Villares, X., 2004. Feasibility Study for a Spacecraft Navigation System Relying on Pulsar Timing Information. Final Report of the Team ARIADNA Study 03/4202, p.32-36.

Sheikh, S.I., 2005. The Use of Variable Celestial X-Ray Sources for Spacecraft Navigation. PhD Thesis, University of Maryland, US, p.220-238.

Sheikh, S.I., Pines, D.J., 2006. Recursive estimation of spacecraft position and velocity using X-ray pulsar time of arrival measurements. *J. Inst. Navig.*, **53**(3):149-166.

Sheikh, S.I., Ray, P.S., Weiner, K., Wolff, M.T., Wood, K.S., 2007. Relative Navigation of Spacecraft Utilizing Bright, Aperiodic Celestial Sources. Proc. 63rd Annual Meeting of the Institute of Navigation, p.444-453.

Tartaglia, A., Ruggiero, M.L., Capolongo, E., 2011. A null frame for spacetime positioning by means of pulsating sources. *Adv. Space Res.*, **47**(4):645-653. [doi:10.1016/j.asr.2010.10.023]

Taylor, J.H., 1992. Pulsar timing and relativistic gravity. *Philosoph. Phil. Trans. R. Soc. Lond. A*, **341**(1660):117-134. [doi:10.1098/rsta.1992.0088]

Woodfork, D.W., Raquet, J.F., Racca, R.A., 2005. Use of X-ray Pulsars for Aiding GPS Satellite Orbit Determination. Proc. 61st Annual Meeting of the Institute of Navigation, p.476-486.

Xiong, K., Wei, C.L., Liu, L.D., 2008. The use of X-ray pulsars for aiding navigation of satellites in constellations. *Acta Astron.*, **64**(4):427-436. [doi:10.1016/j.actaastro.2008.09.005]

Zhang, H., Xu, L.P., 2011. An improved phase measurement method of integrated pulse profile for pulsar. *Sci. China Technol. Sci.*, **54**(9):2263-2270. [doi:10.1007/s11431-011-4524-8]

Zhang, H., Xu, L.P., Xie, Q., 2011a. Modeling and Doppler measurement of X-ray pulsar. *Sci. China Phys. Mech. Astron.*, **54**(6):1068-1076. [doi:10.1007/s11433-011-4338-5]

Zhang, H., Xu, L.P., Xie, Q., 2011b. A search algorithm of phase ambiguity resolution for XPNAV based on binary tree. *Geom. Inf. Sci. Wuhan Univ.*, **36**(1):39-43 (in Chinese).